ACS SENSORS

pubs.acs.org/acssensors

Article

A Label-Free Photoelectrochemical Biosensor Based on CRISPR/Cas12a System Responsive Deoxyribonucleic Acid Hydrogel and "Click" Chemistry

Minghui Liu, Wenxiao Ma, Yanmei Zhou, Bo Liu, Xiaoru Zhang,* and Shusheng Zhang

Cite This: *ACS Sens.* 2022, 7, 3153−3160

Read Online

ACCESS | Metrics & More | Article Recommendations | Supporting Information

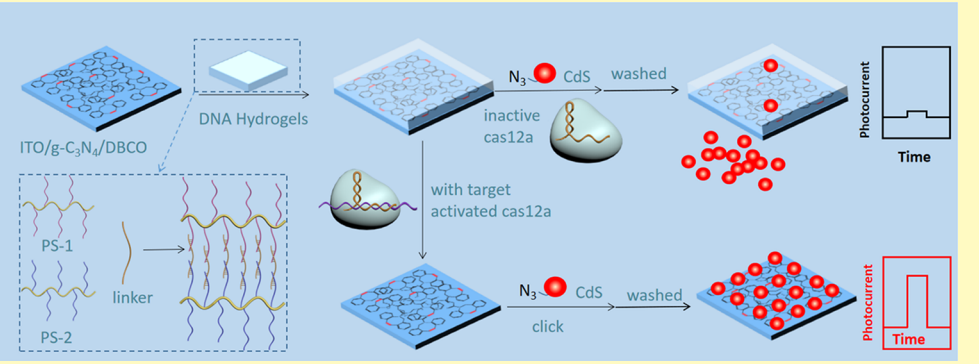

ABSTRACT: A novel label-free photoelectrochemical (PEC) biosensor is presented in this work. As a barrier, the DNA hydrogel could block the coupling between g-C_3N_4 and CdS quantum dots (QDs). Therefore, extremely low photocurrent signals were obtained. The presence of target microRNA-21 can initiate the rolling circle amplification (RCA) reaction, which in turn produces many repeated sequences to activate the CRISPR/Cas12a system. The trans-cleavage activity of the CRISPR/Cas12a system led to the degradation of DNA hydrogels efficiently. As a result, the g-C_3N_4/CdS QDs heterojunction was formed through "click" chemistry. Through the amplification of the RCA and CRISPR/Cas12a system, the sensitivity of the PEC biosensor was improved significantly with the detection limit of 3.2 aM. The proposed sensor also showed excellent selectivity and could be used to detect actual samples. In addition, the modular design could facilitate the detection of different objects. Thus, the proposed CRISPR/Cas12a system responsive DNA hydrogel provides a simple, sensitive, and flexible way for label-free PEC analysis.

KEYWORDS: *CRISPR/Cas12a, DNA hydrogel, PEC biosensor, click chemistry, microRNA-21*

Stimuli-responsive DNA hydrogel networks, including pure DNA and hybrid DNA-polymer hydrogels,[1,2] can change from gel to a sol phase in response to the alteration of external conditions such as pH value, light, temperature, biomolecules, etc.[1,2] Now, the DNA hydrogel has attracted much attention due to its biocompatibility, structural designability, and mechanical stability,[3] which facilitated its application in the field of controlled drug release,[4] tissue engineering,[5] artificial extracellular matrix,[6] and sensing.[7] Based on the unique advantages of DNA recognition followed by the damage to DNA hydrogel structures, various sensors have been developed, including protein,[8,9] small molecule,[10,11] miRNA,[12,13] and metal ion.[14,15] Among these works, the recognition of target and DNA strands in DNA hydrogels is a "one-to-one" pattern with low identification efficiency. To improve the recognition efficiency and expand the detection range, it is necessary to further investigate the application of DNA hydrogel in biosensors.

In recent research, the CRISPR/Cas12a system has attracted much attention because of its excellent performance in gene editing,[16] drug delivery,[17] and biosensors.[18] Among various CRISPR-associated proteins (Cas), Cas12a (Cpf1) is the most eye-catching in the analysis and detection aspects. Under the guidance of CRISPR RNA (crRNA), Cas12a can be activated by target strands with the protospacer adjacent motif (PAM), leading to cis-cleavage and trans-cleavage.[19] Here, cis-cleavage refers to the cleavage of target double-strand DNA (dsDNA). Meanwhile, trans-cleavage means the nonspecific digestion of nearby nontarget ssDNAs. When combined with aptamers, the

Received: July 28, 2022
Accepted: September 29, 2022
Published: October 11, 2022

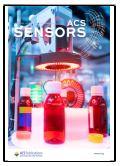

Scheme 1. Schematic Illustration of the Label-Free PEC Sensor Based on the CRISPR/Cas12a System Responsive DNA hydrogel

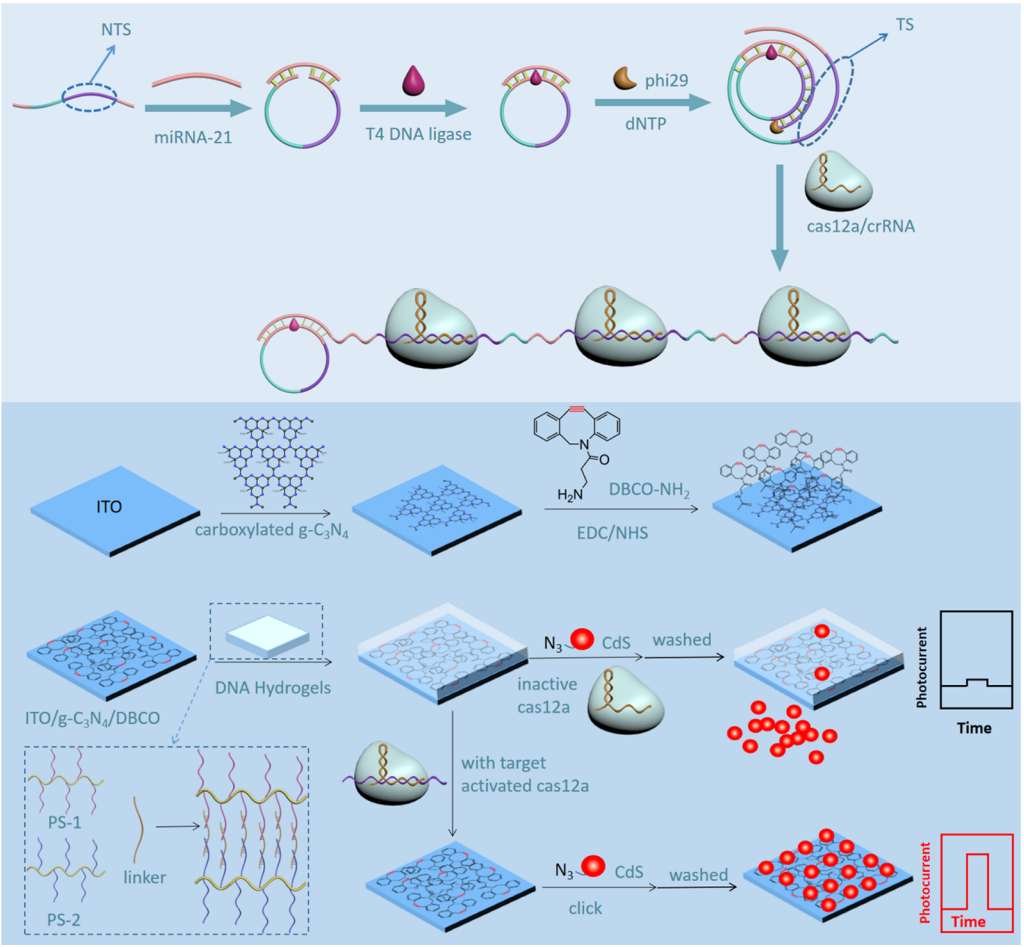

detection range of the CRISPR/Cas12a system can be extended from oligonucleotides[20] to extracellular vesicles,[21] small molecules, and metal ions.[22] Owing to the simplicity, high efficiency, and specificity character of trans-cleavage activity, the CRISPR/Cas12a system has been used in many biosensors, such as fluorescence,[18] colorimetry,[23] surface-enhanced Raman scattering (SERS),[24] electrochemistry,[25] piezoresistors,[26] electrochemiluminescence (ECL),[27] and photoelectrochemistry (PEC).[28]

As an advanced means, the PEC sensor uses optical excitation and electrochemical detection, and thus the signal background is low, which helps to improve the detection sensitivity. Compared to conventional electrochemical and spectroscopic detection, PEC owns the merit of low background signal, high sensitivity, and easy miniaturization.[29−32] At present, there are relatively few reports on PEC sensors based on CRISPR technology.[33,34] Tang's group developed a PEC sensor based on the destruction of (TiO_2)-Au-CdS QDs by activated CRISPR-Cas12a.[35] Hun's group utilized the dsDNA cleavage character of Cas12a, preparing the PEC sensor amplified by redox cycling between $Ru(bpy)_3Cl_2$ and paminophenol.[36] In Liu et al.'s work, dsDNA modified with HPR were fixed on the electrode.[28] After the cis-cleavage of Cas12a, a biocatalytic precipitation (BCP)-based PEC biosensor was obtained.[28] Most of these works, whether they rely on the cis- or trans- cleavage of Cas12a, require a DNA labeling process, which has drawbacks of being time-consuming, having a high cost, and inefficient labeling.

Therefore, the CRISPR/Cas12a-based label-free PEC sensor with an easily accessible sensing interface that increased sensitivity as well as versatility for various analytes is highly deserved.

MicroRNA-21 (miRNA-21), as a member of microRNA family, is often used in early cancer diagnosis due to its overexpression in a variety of tumor cells.[37] In this work, the CRISPR/Cas12a system responsive DNA hydrogel was proposed for PEC detection of miRNA-21 based on "click" chemistry. As shown in Scheme 1, first, carboxyl modified graphitic carbon nitride (g-C_3N_4) was dropped on the surface of the ITO electrode. Then, the dibenzocyclooctyne (DBCO) group was decorated on g-C_3N_4 after condensation with DBCO-NH_2. Subsequently, the prepared DNA hydrogel was added to prevent the contact between azide group-modified CdS QDs (CdS-N_3) and DBCO-C_3N_4/ITO and thereby weakened the PEC signals. In the presence of target miRNA-21, the rolling circle amplification (RCA) reaction could be triggered to produce long DNA amplicons, which could activate the Cas12a, cleave linker ssDNA in the DNA hydrogel, and digest the DNA hydrogel. As a result, CdS-N_3 could react with DBCO-C_3N_4, giving a photoactive CdS@g-C_3N_4 heterojunction. Accordingly, high photocurrent was obtained for PEC detection.

https://doi.org/10.1021/acssensors.2c01636
ACS Sens. 2022, 7, 3153−3160

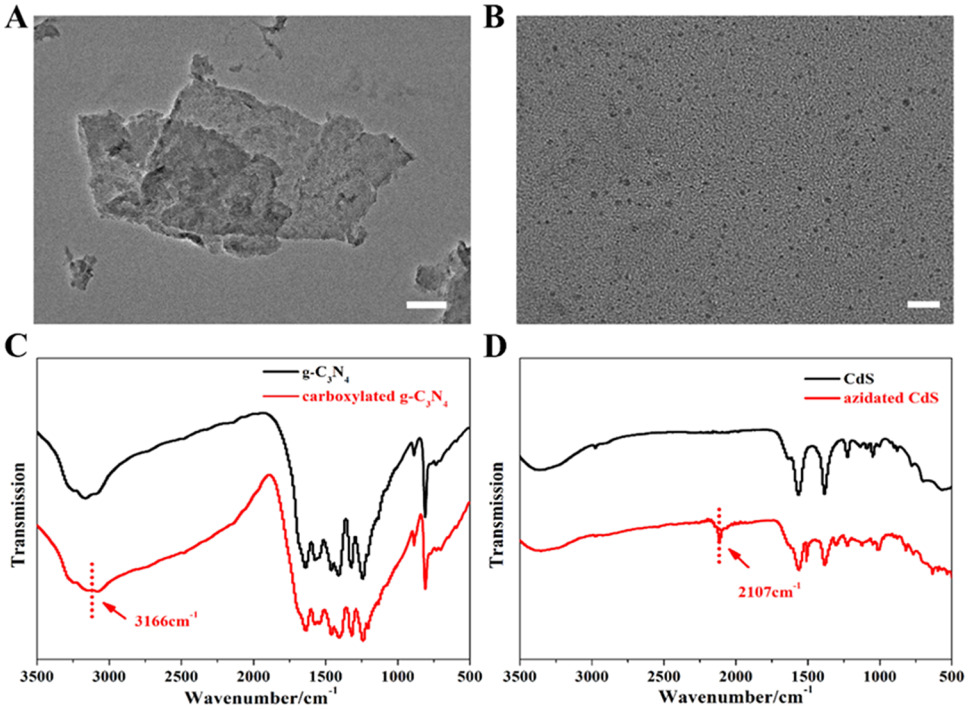

Figure 1. TEM images of (A) carboxylated g-C_3N_4 (scale bar: 200 nm) and (B) CdS QDs (scale bar: 20 nm). IR spectra of (C) g-C_3N_4/carboxylated g-C_3N_4 and (D) CdS QDs/azidated CdS QDs.

Compared with previous works, this work has the following advantages: (1) Unlike "one-to-one" identification in which one target molecule binds and then takes away only one ssDNA in the DNA hydrogel, the activated Cas12a/crRNA can cut off multiple adjacent ssDNA in the DNA hydrogel at the same time. This "one-to-many" recognition results in highly efficient degradation of DNA hydrogels, which can significantly improve the detection sensitivity. (2) Here, the CdS QDS was linked to g-C_3N_4 through an efficient click reaction between N_3 groups and DBCO groups, giving a highly photoelectric active sensing interface. Other efficient recognition events such as streptavidin-biotin have also been widely used.[13,15] Whereas, streptavidin is a protein with high molecular weight and its shielding effect may lead to the reduction of photocurrent. Therefore, the click reaction is more suitable for PEC sensors. (3) The sensor adopts a modular design, whose recognition part is separated from the detection part. When detecting other oligo-nucleotides, only padlock DNA needs to be replaced.

Meanwhile, the Cas12a/crRNA, DNA hydrogel, and assembly of electrodes remain unchanged. When combined with the nucleic acid aptamer, the sensor can also analyze other small molecules or proteins. Consequently, the sensor has good flexibility. (4) The sensor adopts label-free technology and does not need to label DNA with photoelectric active substances. This can reduce the detection cost and save labeling time.

EXPERIMENTAL SECTION

Synthesis of Azidated CdS QDs. The azide modification process of QDs refers to the previous literature.[38] First, 40 mg of CdS QDs (prepared in the Supporting Information) was added to 2 mL of double-distilled water (DDW). After that, 0.1 mmol EDC and 0.1 mmol NHS were added and stirred for 2 h. Subsequently, 2 mL of 0.059 M solution of 4-azidoaniline hydrochloride was introduced and reacted at 25 °C for 24 h. After precipitation with ethanol and washing with methanol, azide group-modified CdS QDs (CdS-N_3) was obtained.

Synthesis of DNA Hydrogels. To a 100 μL mixture containing 10 mM Tris−HCl, 200 mM NaCl, 1 mM EDTA, and 4% acrylamide (pH = 8.0), acrydite-modified DNA-1 and DNA-2 were added. The final concentration of DNA-1 and DNA-2 was 1 μM. These two solutions were degassed in a vacuum oven at 37 °C for 10 min. Then, a 1.4 μL solution containing 0.438 M $(NH_4)_2S_2O_8$ and 0.331 M *N,N,N′,N′*-tetramethylethylenediamine (TEMED) was added. The mixture was degassed in a vacuum oven at 37 °C for 15 min, giving the polymer strands PS1 and PS2, respectively. In order to obtain cross-linked DNA hydrogels, PS1, PS2, and linker DNA were mixed in equal proportions and shook vigorously. After reaction at 50 °C for 5 min and cooling down, the DNA hydrogel was prepared.

Electrode Assembly. Carboxylated g-C_3N_4 (1 mg, prepared in Supporting Information) was ultrasonically dispersed in DDW (1 mL). Then, 40 μL of g-C_3N_4 dispersion was dropped on the pretreated ITO electrode (shown in Supporting Information) and dried under an infrared lamp. After washing with DDW for three times and drying in air, a 10 μL mixture containing 1.0×10^{-2} M EDC and 2.0×10^{-2} M NHS was added to g-C_3N_4/ITO. The electrode was left at room temperature and washed before it was completely dried. Subsequently, 10 μL of 100 μg·mL^{-1} DBCO-NH_2 was dropped on the electrode and then incubated at 4 °C for 1 h, followed by rinsing off physically absorbed DBCO-NH_2 to give the g-C_3N_4-DBCO-modified ITO electrode. Finally, 10 μL of prepared DNA hydrogel was evenly added to the electrode and dried naturally.

RCA Reaction. First, in 1 × T4 DNA ligase buffer, 10 μM padlock DNA and various concentrations of miRNA-21 were annealed at 95 °C for 5 min and then naturally cooled down. After that, T4 DNA ligase was added to make the final concentration of 10 U/μL. The reactants were incubated at 16 °C for 2 h and heated at 65 °C for 10 min to denature the ligase. Further, phi29 DNA polymerase (final concentration: 1 U/μL), 1× phi29 DNA polymerase buffer, 2 mM dNTP, and 1× BSA were added to 10 μL of the above reaction solution. After reaction at 30 °C for 2 h, a long-chain RCA product with repeated sequences for the activation of Cas12a/crRNA was obtained. Oligonucleotides used in this step were diluted with DEPC water.

https://doi.org/10.1021/acssensors.2c01636
ACS Sens. 2022, 7, 3153−3160

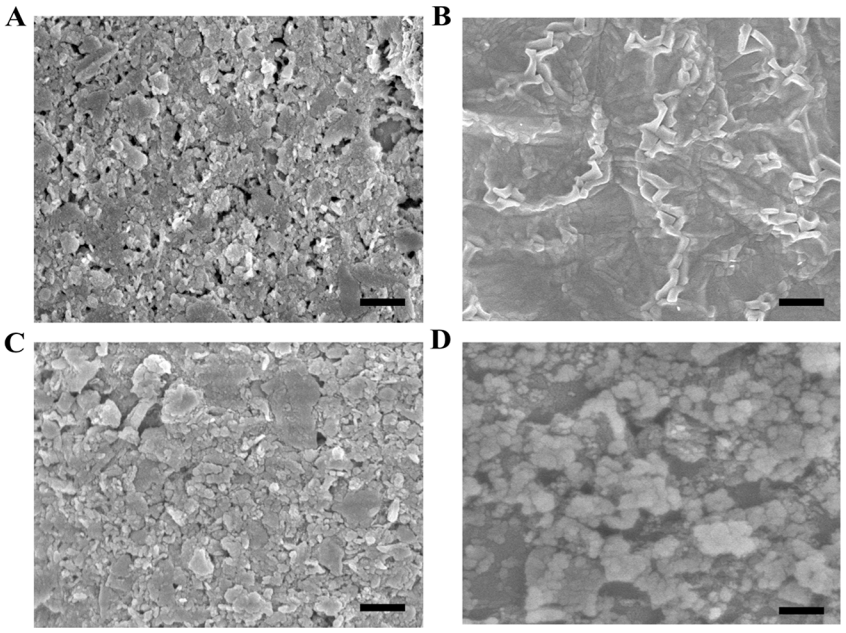

Figure 2. SEM images of (A) g-C_3N_4-DBCO-modified ITO electrode; (B) added DNA hydrogel on (A); (C) added activated Cas12a/crRNA to (B); (D) added CdS-N_3 to (C). The electrodes were washed after each assembly. Scale bar: 1 μm.

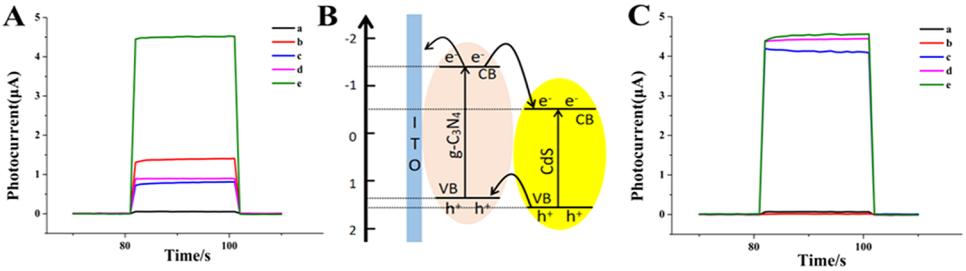

Figure 3. (A) Photocurrent response of the ITO electrode modified with (a) g-C_3N_4, (b) CdS, (c) g-C_3N_4-DBCO+CdS, (d) g-C_3N_4 + CdS-N_3, and (e) g-C_3N_4-DBCO+CdS-N_3. (B) Electron-transfer process of the g-C_3N_4/CdS heterojunction. (C) PEC characterization of (a) g-C_3N_4/hy/CdS + Cas12a, (b) g-C_3N_4/hy/CdS, (c) g-C_3N_4/PS1 + PS2/CdS, (d) g-C_3N_4/hy/CdS + Cas12a + activator ssDNA, and (e) g-C_3N_4/CdS.

CRISPR/Cas12a Activation and the Reaction on the Electrode. The CRISPR/Cas12a system (27 μL) containing 17 μL of DEPC water, 37 nM Cas12a, 74 nM crRNA, 1 × NEB buffer 2.1, 2.96 U/μL of RNase inhibitor, and 2 μL of RCA product was dropped onto the DNA hydrogel-modified electrode and incubated at 37 °C for 1 h in a humid environment. Then, the Cas12a enzyme was washed away with PBS containing 1% Tween. Finally, 40 μL of 1.5 mg/mL CdS-N_3 was dropped on the electrode and incubated for 0.5 h. Physically adsorbed CdS QDs were washed away with PBS.

Photoelectrochemical Detection. PEC detection was performed in PBS (pH 7.4) containing 0.1 M ascorbic acid (AA). The bias voltage was 0 V, and the light wavelength was 430 nm with an intensity of 180 W·m^{-2}.

RESULTS AND DISCUSSION

Material Characterization. The TEM image of carboxylated g-C_3N_4 showed a typical nanosheet structure (Figure 1A). For cadmium sulfide, TEM indicated that the quantum dots were about 4 nm in size (Figure 1B). The X-ray diffraction (XRD) patterns of g-C_3N_4 and CdS QDs were shown in Figure S1. Two peaks at 13.1 and 27.5° (red curve) were assigned to the (100) and (002) diffraction planes of g-C_3N_4. Meanwhile, three diffraction peaks at 26.4, 43.6, and 51.8° (black curve) were attributed to the (111), (220), and (311) planes of CdS QDs, respectively. The FT-IR spectra were used to verify the modification of g-C_3N_4 (Figure 1C) and CdS (Figure 1D). Compared to pure g-C_3N_4 (black curve in 1C), carboxylated g-C_3N_4 showed stronger band intensity at 2500−3200 cm^{-1} caused by the stretching vibration of the associated hydroxyl group (red curve in Figure 1C). On the other hand, compared to CdS QDs (black curve in Figure 1D), the peak at 2107 cm^{-1} is the stretching vibration of the $-N_3$ group (red curve in Figure 1D), indicating the successful preparation of modification of the azide group on CdS QDs.

To synthesize a 3D DNA hydrogel, linker DNA hybridized with DNA-1 and DNA-2 was grafted on PS-1 and PS-2, respectively, giving a 3D network-like DNA hydrogel. The hybridization of linker DNA with DNA-1 and DNA-2 was verified by polyacrylamide gel electrophoresis (Figure S2). Additionally, compared to linear polymer PS-1 and PS-2, the zeta potential of the prepared DNA hydrogel was more negative (Figure S3), suggesting the presence of many negatively charged DNA strands.

The assembly process on the electrode was characterized by scanning electron microscopy (SEM). As shown in Figure 2A, the g-C_3N_4 modified ITO electrode showed a stacked layered structure. After adding DNA hydrogels, the dense structure of the hydrogel was found, which could block the click reaction between g-C_3N_4 and CdS QDs and prevent the electron transfer between g-C_3N_4 and CdS QDs (Figure 2B). After the

https://doi.org/10.1021/acssensors.2c01636
ACS Sens. 2022, 7, 3153−3160

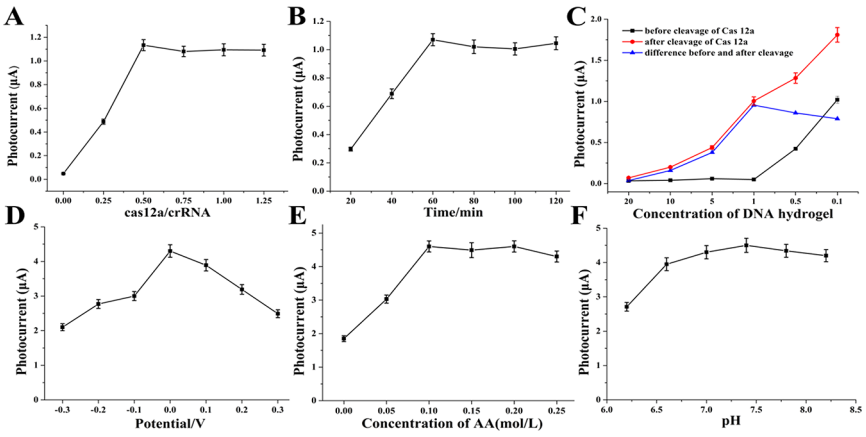

Figure 4. Optimization of experimental conditions. (A) Ratio of Cas12a to crRNA; (B) reaction time for the CRISPR/Cas12a system; (C) concentration of the DNA hydrogel; (D) bias potential for PEC detection; (E) concentration of AA for PEC detection; (F) pH value for PEC detection.

cleavage of the DNA hydrogel on the electrode by activated Cas12a/crRNA and washing the electrode, the layered structure of g-C_3N_4 was restored (Figure 2C). Figure 2D shows the uniform granular structure of CdS QDs on the g-C_3N_4 sheet surface, suggesting that the click reaction occurred between g-C_3N_4-DBCO and CdS-N_3.

Validation Feasibility. In order to verify the detection feasibility of the developed method, several control experiments were performed. The PEC analysis was performed in 0.1 M PBS containing 0.1 M AA under 430 nm light irradiation. As seen from Figure 3A, g-C_3N_4-modified ITO showed a weak photocurrent (curve a). As for the CdS QD-modified ITO electrode, a higher PEC response was obtained (curve d). Then, non-azided CdS QDs were added to g-C_3N_4-DBCO on the ITO electrode. After incubation for 1 h and washing the electrode, the photocurrent enhanced slightly compared with that of the g-C_3N_4 modified electrode because of the physical adsorption of CdS QDs (curve b). Similar weak signals were observed when adding CdS-N_3 to g-C_3N_4 without the modification of DBCO (curve c). Nevertheless, when CdS-N_3 was added to g-C_3N_4-DBCO on the ITO electrode, a much higher photocurrent was obtained after incubation for 1 h and washing the electrode (curve d). This demonstrated that CdS QDs could connect to g-C_3N_4 effectively through the click reaction, and the prepared g-C_3N_4/CdS composite showed a strong photoelectrical response. The energy band structure of the g-C_3N_4/CdS composite is shown in Figure 3B. Due to the well-matched band structure, g-C_3N_4 and CdS QDs could form a heterojunction, which facilitated an efficient charge transfer and impeded the recombination of electrons and holes. Accordingly, an enhanced photocurrent signal was observed.

As indicated in Figure 3C, compared to the g-C_3N_4/CdS composite-modified ITO electrode (curve e), when introducing the DNA hydrogel between g-C_3N_4 and CdS QDs, the photocurrent of g-C_3N_4/hy/CdS decreased dramatically (curve b). This can be explained as the existence of a 3D network DNA hydrogel blocking the touch between g-C_3N_4 and CdS, so the heterojunction structure could not form. If polymer strands PS1 and PS2 were added to the electrode without linker DNA, a porous network structure could not form. Therefore, a higher photocurrent signal was found (curve c). When Cas12a/crRNA solution was added to the electrode modified with g-C_3N_4/hy/CdS, the photocurrent was still very low. However, after adding the mixture of Cas12a/crRNA and 1.0×10^{-6} activator TS DNA to the g-C_3N_4/hy/CdS-modified electrode, the activated Cas12a cut linker DNA in the DNA hydrogel network because of the nonspecific trans-cleavage activity. The breakdown of the DNA hydrogel could not prevent the click reaction between g-C_3N_4-DBCO and CdS-N_3. Therefore, a much stronger photocurrent signal was obtained because of the formation of the g-C_3N_4/CdS heterojunction.

Subsequently, the electrochemical impedance spectroscopy (EIS) of each assembly step on the surface of the ITO electrode was investigated. As shown in Figure S4, the impedance value increased significantly with the introduction of nanomaterials on the electrode surface. The impedance value was the greatest when g-C_3N_4 was coupled to CdS QDs by the click reaction (curve d). Meanwhile, the addition of DNA hydrogels had less effect on the impedance (curves c and e). However, the disruption of the DNA hydrogel by activated Cas12a increased the amount of CdS QDs coupled on the electrode surface, which led to an increase in impedance values (curve f). This indicated that the assembly of the electrodes was successful. In addition, the trans-cleavage activity of Cas12a could also be verified by the cleavage of fluorophore and quencher-labeled ssDNA (FQ) reporters (Figure S5).

To further improve the detection sensitivity, the RCA reaction was applied to produce more activator DNA. The progress of RCA could be confirmed by polyacrylamide gel electrophoresis (Figure S6). The brightest band at the top of lane 5 represented RCA products. The amplification effect of RCA could be demonstrated by the PEC experiment. As shown in Figure S7, the photocurrent produced by 1.0×10^{-9} M target miRNA-21 after the RCA reaction (red curve) is similar to that of 1.0×10^{-6} M activator TS DNA without RCA (black curve). Meanwhile, the photocurrent produced by 1.0×10^{-9} M TS DNA without RCA is much lower (blue curve). This indicates that the low concentration of the target miRNA-21 generates long-chain products with repeated sequences after the RCA reaction, which produces multiple activator DNA for the activation of Cas12a/crRNA.

Optimization of Experiment Conditions. This experiment is divided into two modules: one is the RCA reaction and Cas12a activation part and the other is the PEC detection part. As for the enzymatic reaction catalyzed by Cas12a/crRNA, the ratio of Cas12a to crRNA and the enzyme cutting time were investigated. As indicated in Figure 4A,B, in the presence of 1.0

https://doi.org/10.1021/acssensors.2c01636
ACS Sens. 2022, 7, 3153−3160

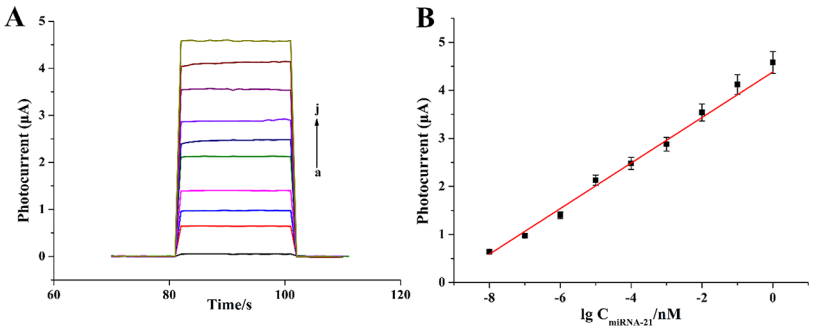

Figure 5. (A) Photocurrent response to different concentrations of miRNA-21 from a to j: 0, 1.0×10^{-17}, 1.0×10^{-16}, 1.0×10^{-15}, 1.0×10^{-14}, 1.0×10^{-13}, 1.0×10^{-12}, 1.0×10^{-11}, 1.0×10^{-10}, and 1.0×10^{-9} M. (B) Calibration plot between photocurrent and the logarithm of miRNA-21 concentration (nM).

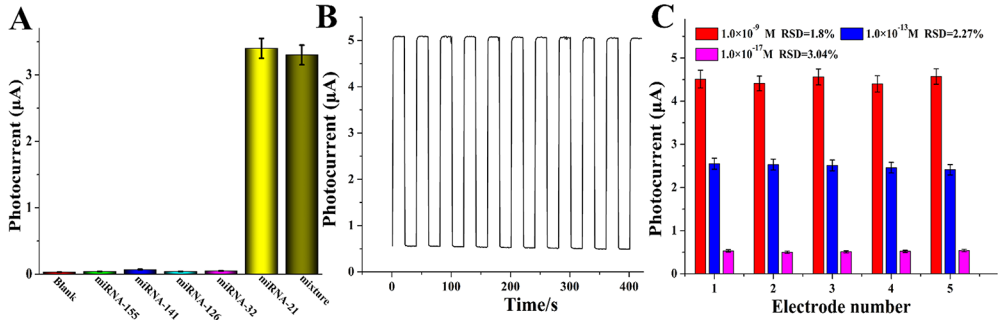

Figure 6. (A) Specificity of developed PEC sensor toward various interferences. (B) Stability of photocurrent within 400 s in response to 1.0×10^{-9} M miRNA-21. (C) Reproducibility of five parallel experiments at three concentrations.

$\times 10^{-16}$ M miRNA-21, the optimal PEC signals were obtained when the ratio of Cas12a to crRNA was 0.5:1 and the incubation time was 1 h.

The concentration of the DNA hydrogel occupies a significant position in PEC detection. A high concentration of DNA hydrogel will consume too many Cas12a for opening the reaction pathway, which can decrease the detection sensitivity. When the concentration of the DNA hydrogel is too low, the photoelectric sensing interface cannot be well covered, leading to the increase of background signal. As indicated in Figure 4C, with the decrease of DNA hydrogel concentration, the photocurrent signals after the cleavage of Cas12a/crRNA increased steadily, while the background signals before the cleavage of Cas12a/crRNA suddenly increased when the hydrogel concentration was lower than 1.0 μM (the concentration of target miRNA-21 is 1.0×10^{-16} M). Considering the change of photocurrent signals before and after the cleavage of Cas12a/crRNA, 1 μM DNA hydrogel was selected to give the best signal-to-noise ratio. Such concentration is much lower than previous studies where DNA hydrogels were used for embedding.[7,39]

During the electrode assembly process, the amount of g-C_3N_4 was optimized. From the results in the Figure S8, it could be seen that the optimal concentration of g-C_3N_4 was 1.0 mg/mL. Then, detection bias potential was compared in Figure 4D. From the result, we could see that 0 V bias potential produced the biggest photocurrent. As we all know, the self-powered PEC sensor without bias voltage can avoid the interference of environmental pollutants and improve the anti-pollution ability, which is also a significant advantage of this sensor. Subsequently, the concentration of electron donor AA and pH of buffer were optimized. From the results shown in Figure 4,FE, we selected 0.1 M AA and pH 7.4 PBS as the optimal conditions in the following experiments.

Analytical Performance. Under the optimal conditions, the photocurrent responses for different amounts of miRNA-21 s were examined. As indicated in Figure 5A, the photocurrent signal rose steadily with the increase of miRNA-21 concentration from 10 aM to 1 nM. The photocurrent intensity showed a linear relationship to the logarithm of miRNA-21 concentrations from 10 aM to 1 nM (Figure 5B). The linear regression equation was I (μA) = 4.38 + 0.47lgC (nM) (R^2 = 0.995), and the detection limit was estimated to be 3.2 aM (S/N = 3). In comparison with previous reports for miRNA-21 detection, the developed Cas12a/crRNA based PEC sensor exhibits superior detection performance (Table S2).

For evaluating the detection specificity, four kinds of miRNAs, including miRNA-155, miRNA-141, miRNA-126, and miRNA-32 were selected as interferences for comparison with the miRNA-21. As displayed in Figure 6A, the PEC signals produced by interfering miRNAs (1 nM) were identical to that of the blank group. Instead, miRNA-21 (10 pM) produced a significant PEC signal. As for the mixture of miRNA-21 with interferences, the signal intensity was almost identical to that of miRNA-21 alone. This suggested that the developed sensor has a good selectivity as well as strong anti-interference performance.

The sensor stability was determined by measuring the photocurrent signal in the presence of 1.0×10^{-9} M miRNA-21 under 10 times successive on−off−on light cycles. The result shown in Figure 6B suggested no significant change in the photocurrent signals during 400 s of measurement.

To test the storage stability of the prepared sensor, six parallel electrodes modified with g-C_3N_4 and DNA hydrogels

https://doi.org/10.1021/acssensors.2c01636
ACS Sens. 2022, 7, 3153−3160

were placed in a 4 °C refrigerator. The modified electrodes were treated with activated Cas12a every 3 days before reacting with modified azide-linked CdS QDs, followed by photoelectrical measurement. As could be seen from the results in Figure S9, after 15 days of storage, there was only a slight decrease in the photocurrent signal and the signal intensity could reach 90.7% of the original value, which indicated that the prepared electrodes had good storage stability.

The reproducibility was demonstrated by five sets of parallel experiments. Three different concentrations of miRNA-21 s (1.0×10^{-9}, 1.0×10^{-13}, and 1.0×10^{-17} M) were selected in each group. As shown in Figure 6C, the relative standard deviation (RSD) was less than 3.04%, indicating the excellent reproducibility of the fabricated PEC biosensor.

Application of Developed PEC Sensors in Cell Lysates Assays. To investigate the application of developed PEC sensor for a real sample, cell lysates of breast adenocarcinoma cells (MCF-7) with high miRNA-21 expression and human cervical cancer cells (Hela) with low miRNA-21 expression were detected. After counting the cultured cells, total RNA was extracted with a Trizol Reagent Kit. According to Figure 7, the photocurrent intensity gradually increased as the number of cells increased from 10 to 10^5. Notably, the photocurrent intensity of MCF-7 cell extracts was significantly higher than that of Hela cells, and the increase in photocurrent of MCF-7 cell extracts was more significant as the number of cells increased. This finding is in agreement with previous studies reported,[40,41] which also confirms that the sensor can be applied in the analysis of complex systems.

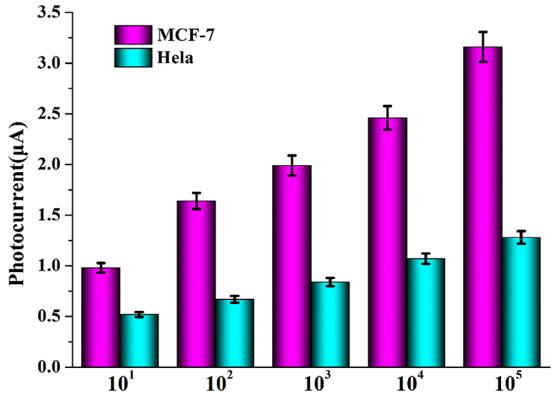

Figure 7. Detection of miRNA-21 in MCF-7 and Hela cell lysates using the developed PEC sensor.

CONCLUSIONS

In summary, a PEC biosensor based on a CRISPR/Cas12a responsive DNA hydrogel was developed for miRNA-21 detection. This work consists of two modules. One is the target recognition, RCA, and CRISPR/Cas12a activation part. The other is the PEC analysis part based on a DNA hydrogel. Different targets can be detected only by replacing different padlock DNA strands, so this sensor owns the merit of good flexibility. The highly efficient trans-cleavage activity of CRISPR/Cas12a system can improve the detection sensitivity significantly. The developed sensor adopts the label-free technology to obtain an efficient photoelectric sensing interface through the click reaction, which provides a new avenue for label-free PEC sensors.

ASSOCIATED CONTENT

Supporting Information

The Supporting Information is available free of charge at https://pubs.acs.org/doi/10.1021/acssensors.2c01636.

Materials, instrument, experimental details, additional XRD of g-C_3N_4 and CdS, polyacrylamide gel electrophoresis, zeta potential, and amplification effect of RCA (PDF)

AUTHOR INFORMATION

Corresponding Author

Xiaoru Zhang − *Key Laboratory of Optic-electric Sensing and Analytical Chemistry for Life Science, MOE; Shandong Key Laboratory of Biochemical Analysis, Qingdao University of Science and Technology, Qingdao 266042, P.R. China;* orcid.org/0000-0002-2251-3208; Email: zhangxr7407@126.com

Authors

Minghui Liu − *College of Chemistry and Chemical Engneering, Linyi University, Linyi 276000, P.R. China*

Wenxiao Ma − *College of Chemistry and Chemical Engneering, Linyi University, Linyi 276000, P.R. China*

Yanmei Zhou − *College of Chemistry and Chemical Engneering, Linyi University, Linyi 276000, P.R. China*

Bo Liu − *College of Chemistry and Chemical Engneering, Linyi University, Linyi 276000, P.R. China*

Shusheng Zhang − *Shandong Province Key Laboratory of Detection Technology for Tumor Makers, Collaborative Innovation Center of Tumor Marker Detection Technology, Equipment and Diagnosis-Therapy Integration in Universties of Shandong and College of Chemistry and Chemical Engneering, Linyi University, Linyi 276000, P.R. China*

Complete contact information is available at: https://pubs.acs.org/10.1021/acssensors.2c01636

Author Contributions

The manuscript was written through contributions of all authors. All authors have given approval to the final version of the manuscript.

Notes

The authors declare no competing financial interest.

ACKNOWLEDGMENTS

This work was financially supported by the National Natural Science Foundation of China (nos. 22276103, 21775080, and 22076073).

REFERENCES

(1) Li, J.; Mo, L.; Lu, C.-H.; Fu, T.; Yang, H.-H.; Tan, W. Functional nucleic acid-based hydrogels for bioanalytical and biomedical applications. *Chem. Soc. Rev.* **2016**, *45*, 1410−1431.

(2) Kahn, J. S.; Hu, Y.; Willner, I. Stimuli-Responsive DNA-Based Hydrogels: From Basic Principles to Applications. *Acc. Chem. Res.* **2017**, *50*, 680−690.

(3) Wang, C.; Zhang, J. Recent Advances in Stimuli-Responsive DNA-Based Hydrogels. *ACS Appl. Bio Mater.* **2022**, *5*, 1934−1953.

(4) Hu, Y.; Gao, S.; Lu, H.; Ying, J. Y. Acid-Resistant and Physiological pH-Responsive DNA Hydrogel Composed of A-Motif and i-Motif toward Oral Insulin Delivery. *J. Am. Chem. Soc.* **2022**, *144*, 5461−5470.

(5) Wang, Y.; Shao, Y.; Ma, X.; Zhou, B.; Faulkner-Jones, A.; Shu, W.; Liu, D. Constructing Tissuelike Complex Structures Using Cell-

Laden DNA Hydrogel Bricks. *ACS Appl. Mater. Interfaces* **2017**, *9*, 12311−12315.
(6) Wei, Y.; Wang, K.; Luo, S.; Li, F.; Zuo, X.; Fan, C.; Li, Q. Programmable DNA Hydrogels as Artificial Extracellular Matrix. *Small* **2022**, *18*, 2107640.
(7) Zhu, Z.; Wu, C.; Liu, H.; Zou, Y.; Zhang, X.; Kang, H.; Yang, C. J.; Tan, W. An Aptamer Cross-Linked Hydrogel as a Colorimetric Platform for Visual Detection. *Angew. Chem., Int. Ed.* **2010**, *49*, 1052−1056.
(8) Zhang, L.; Lei, J.; Liu, L.; Li, C.; Ju, H. Self-Assembled DNA Hydrogel as Switchable Material for Aptamer-Based Fluorescent Detection of Protein. *Anal. Chem.* **2013**, *85*, 11077−11082.
(9) Gao, X.; Li, X.; Sun, X.; Zhang, J.; Zhao, Y.; Liu, X.; Li, F. *Anal. Chem.* **2020**, *92*, 4592−4599.
(10) Lin, Y.; Wang, X.; Sun, Y.; Dai, Y.; Sun, W.; Zhu, X.; Liu, H.; Han, R.; Gao, D.; Luo, C. A chemiluminescent biosensor for ultrasensitive detection of adenosine based on target-responsive DNA hydrogel with Au@HKUST-1 encapsulation. *Sen. Actuators, B* **2019**, *289*, 56−64.
(11) Zeng, R.; Huang, Z.; Wang, Y.; Tang, D. Enzyme-Encapsulated DNA Hydrogel for Highly Efficient Electrochemical Sensing Glucose. *ChemElectroChem* **2020**, *7*, 1537−1541.
(12) He, Y.; Yang, X.; Yuan, R.; Chai, Y. Switchable Target-Responsive 3D DNA Hydrogels As a Signal Amplification Strategy Combining with SERS Technique for Ultrasensitive Detection of miRNA 155. *Anal. Chem.* **2017**, *89*, 8538−8544.
(13) Si, Y.; Xu, L.; Wang, N.; Zheng, J.; Yang, R.; Li, J. Target MicroRNA-Responsive DNA Hydrogel-Based Surface-Enhanced Raman Scattering Sensor Arrays for MicroRNA-Marked Cancer Screening. *Anal. Chem.* **2020**, *92*, 2649−2655.
(14) Liu, C.; Gou, S.; Bi, Y.; Gao, Q.; Sun, J.; Hu, S.; Guo, W. Smart DNA-gold nanoparticle hybrid hydrogel film based portable, cost-effective and storable biosensing system for the colorimetric detection of lead (II) and uranyl ions. *Biosens. Bioelectron.* **2022**, *210*, 114290.
(15) He, X.; Zhou, X.; Liu, W.; Liu, Y.; Wang, X. Flexible DNA Hydrogel SERS Active Biofilms for Conformal Ultrasensitive Detection of Uranyl Ions from Aquatic Products. *Langmuir* **2020**, *36*, 2930−2936.
(16) Hsu, P. D.; Lander, E. S.; Zhang, F. Development and Applications of CRISPR-Cas9 for Genome Engineering. *Cell* **2014**, *157*, 1262−1278.
(17) Ma, Y.; Mao, G.; Wu, G.; Cui, Z.; Zhang, X.-E.; Huang, W. CRISPR-dCas9-Guided and Telomerase-Responsive Nanosystem for Precise Anti-Cancer Drug Delivery. *ACS Appl. Mater. Interfaces* **2021**, *13*, 7890−7896.
(18) Peng, S.; Tan, Z.; Chen, S.; Lei, C.; Nie, Z. Integrating CRISPR-Cas12a with a DNA circuit as a generic sensing platform for amplified detection of microRNA. *Chem. Sci.* **2020**, *11*, 7362−7368.
(19) Chen, J. S.; Ma, E.; Harrington, L. B.; Costa, M. D.; Tian, X.; Palefsky, J.; Doudna, J. A. CRISPR-Cas12a target binding unleashes indiscriminate single-stranded DNase activity. *Science* **2018**, *360*, 436−439.
(20) Wang, G.; Tian, W.; Liu, X.; Ren, W.; Liu, C. New CRISPR-Derived microRNA Sensing Mechanism Based on Cas12a Self-Powered and Rolling Circle Transcription-Unleashed Real-Time crRNA Recruiting. *Anal. Chem.* **2020**, *92*, 6702−6708.
(21) Zhao, X.; Zeng, L.; Mei, Q.; Luo, Y. Allosteric Probe-Initiated Wash-Free Method for Sensitive Extracellular Vesicle Detection through Dual Cycle-Assisted CRISPR-Cas12a. *ACS Sens.* **2020**, *5*, 2239−2246.
(22) Xiong, Y.; Zhang, J.; Yang, Z.; Mou, Q.; Ma, Y.; Xiong, Y.; Lu, Y. Functional DNA Regulated CRISPR-Cas12a Sensors for Point-of-Care Diagnostics of Non-Nucleic-Acid Targets. *J. Am. Chem. Soc.* **2020**, *142*, 207−213.
(23) Li, Y.; Mansour, H.; Wang, T.; Poojari, S.; Li, F. Naked-Eye Detection of Grapevine Red-Blotch Viral Infection Using a Plasmonic CRISPR Cas12a Assay. *Anal. Chem.* **2019**, *91*, 11510−11513.
(24) Choi, J. H.; Shin, M.; Yang, L.; Conley, B.; Yoon, J.; Lee, S. N.; Lee, K. B.; Choi, J. W. Clustered Regularly Interspaced Short Palindromic Repeats-Mediated Amplification-Free Detection of Viral DNAs Using Surface-Enhanced Raman Spectroscopy-Active Nanoarray. *ACS Nano* **2021**, *15*, 13475−13485.
(25) Zhang, D.; Yan, Y.; Que, H.; Yang, T.; Cheng, X.; Ding, S.; Zhang, X.; Cheng, W. CRISPR/Cas12a-Mediated Interfacial Cleaving of Hairpin DNA Reporter for Electrochemical Nucleic Acid Sensing. *ACS Sens.* **2020**, *5*, 557−562.
(26) Zeng, R.; Wang, W.; Chen, M.; Wan, Q.; Wang, C.; Knopp, D.; Tang, D. CRISPR-Cas12a-driven MXene-PEDOT:PSS piezoresistive wireless biosensor. *Nano Energy* **2021**, *93*, 105711−105720.
(27) Wang, Q.; Liu, Y.; Yan, J.; Liu, Y.; Gao, C.; Ge, S.; Yu, J. 3D DNA Walker-Assisted CRISPR/Cas12a Trans-Cleavage for Ultrasensitive Electrochemiluminescence Detection of miRNA-141. *Anal. Chem.* **2021**, *93*, 13373−13381.
(28) Shen, H.; Qileng, A.; Yang, H.; Liang, H.; Zhu, H.; Liu, Y.; Lei, H.; Liu, W. "Dual-Signal-On" Integrated-Type Biosensor for Portable Detection of miRNA: Cas12a-Induced Photoelectrochemistry and Fluorescence Strategy. *Anal. Chem.* **2021**, *93*, 11816−11825.
(29) Zhao, W.-W.; Xu, J.-J.; Chen, H.-Y. Photoelectrochemical bioanalysis: the state of the art. *Chem. Soc. Rev.* **2015**, *44*, 729−741.
(30) Gao, Y.; Zeng, Y.; Liu, X.; Tang, D. Liposome-Mediated In Situ Formation of Type-I Heterojunction for Amplified Photoelectrochemical Immunoassay. *Anal. Chem.* **2022**, *94*, 4859−4865.
(31) Shu, J.; Tang, D. Recent Advances in Photoelectrochemical Sensing: From Engineered Photoactive Materials to Sensing Devices and Detection Modes. *Anal. Chem.* **2020**, *92*, 363−377.
(32) Zhou, Q.; Tang, D. Recent advances in photoelectrochemical biosensors for analysis of mycotoxins in food. *Trend Anal. Chem.* **2020**, *124*, 115814−115825.
(33) Zeng, R.; Gong, H.; Li, Y.; Li, Y.; Lin, W.; Tang, D.; Knopp, D. CRISPR-Cas12a-Derived Photoelectrochemical Biosensor for Point-Of-Care Diagnosis of Nucleic Acid. *Anal. Chem.* **2022**, *94*, 7442−7448.
(34) Gong, H.; Wu, Y.; Zeng, R.; Zeng, Y.; Liu, X.; Tang, D. CRISPR/Cas12a-mediated liposome-amplified strategy for the photoelectrochemical detection of nucleic acid. *Chem. Commun.* **2021**, *57*, 8977−8980.
(35) Li, Y.; Zeng, R.; Wang, W.; Xu, J.; Gong, H.; Li, L.; Li, M.; Tang, D. Size-Controlled Engineering Photoelectrochemical Biosensor for Human Papillomavirus-16 Based on CRISPR-Cas12a-Induced Disassembly of Z-Scheme Heterojunctions. *ACS Sens.* **2022**, *7*, 1593−1601.
(36) Qin, N.; Deng, L.; Wang, M.; Hun, X. Gold Nanoparticles/Mo2C/MoO2-Modified Electrodes for Nucleic Acid Detection through CRISPR/Cas12a Photoelectrochemical Assay. *ACS Appl. Nano Mater.* **2021**, *4*, 10701−10707.
(37) Kong, L.; Li, H.; Zhang, X.; Zhuo, Y.; Chai, Y.; Yuan, R. A Novel Ratiometric Electrochemical Biosensor Using Only One Signal Tag for Highly Reliable and Ultrasensitive Detection of miRNA-21. *Anal. Chem.* **2022**, *94*, 5167−5172.
(38) Nxele, S. R.; Nyokong, T. Conjugation of Azide-functionalised CdSe/ZnS Quantum Dots with Tetrakis(5-hexyn-oxy) Fe(II) phthalocyanine via Click Chemistry for Electrocatalysis. *Electrochim. Acta* **2016**, *194*, 26−39.
(39) Jiang, C.; Wang, F.; Zhang, K.; Min, T.; Chen, D.; Wen, Y. Distance-Based Biosensor for Ultrasensitive Detection of Uracil-DNA Glycosylase Using Membrane Filtration of DNA Hydrogel. *ACS Sens.* **2021**, *6*, 2395−2402.
(40) Gong, X.; Li, R.; Wang, J.; Wei, J.; Ma, K.; Liu, X.; Wang, F. A Smart Theranostic Nanocapsule for Spatiotemporally Programmable Photo-Gene Therapy. *Angew. Chem., Int. Ed.* **2020**, *59*, 21648−21655.
(41) Liu, W.; Su, M.; Chen, A.; Peng, K.; Chai, Y.; Yuan, R. Highly Efficient Electrochemiluminescence Based on Luminol/MoS2 Quantum Dots@Zeolitic Imidazolate Framework-8 as an Emitter for Ultrasensitive Detection of MicroRNA. *Anal. Chem.* **2022**, *94*, 9106−9113.

https://doi.org/10.1021/acssensors.2c01636
ACS Sens. 2022, 7, 3153−3160